

Received: 2018.11.13
Accepted: 2019.02.21
Published: 2019.03.16

Cardiac Sympathetic Afferent Denervation Protects Against Ventricular Arrhythmias by Modulating Cardiac Sympathetic Nerve Activity During Acute Myocardial Infarction

Authors' Contribution:
Study Design A
Data Collection B
Statistical Analysis C
Data Interpretation D
Manuscript Preparation E
Literature Search F
Funds Collection G

ABCDEF G 1,2,3 **Mingmin Zhou**
ABEFG 1,2,3 **Yu Liu**
ABC 1,2,3 **Liang Xiong**
AB 1,2,3 **Dajun Quan**
BC 1,2,3 **Yan He**
AG 1,2,3 **Yanhong Tang**
AG 1,2,3 **He Huang**
ABG 1,2,3 **Congxin Huang**

1 Department of Cardiology, Renmin Hospital of Wuhan University, Wuhan, Hubei, P.R. China
2 Cardiovascular Research Institute of Wuhan University, Wuhan, Hubei, P.R. China
3 Hubei Key Laboratory of Cardiology, Wuhan, Hubei, P.R. China

Corresponding Author: Yu Liu, e-mail: liuyu1983@whu.edu.cn
Source of support: This work was supported by grants from the National Natural Science Foundation of China (No. 81570459)

Background: Augmented cardiac sympathetic afferent reflex (CSAR) plays a role in enhanced sympathetic activity. Given that a strategy for abolishing augmented CSAR-induced sympathetic activation may be beneficial for protecting against ventricular arrhythmias (VAs) triggered by acute myocardial infarction (AMI), we investigated whether cardiac sympathetic afferent denervation (CSAD) could protect against VAs by modulating cardiac sympathetic nerve activity in an AMI dog model.

Material/Methods: Twenty-two anesthetized dogs were assigned to the CSAD group (n=9) and the sham group (n=13) randomly. CSAD was produced by epicardial application of resineratoxin. Heart rate variability (HRV), ventricular action potential duration (APD), APD dispersion, beat-to-beat variability of repolarization (BVR), effective refractory period (ERP) of ventricles, ERP dispersion, plasma norepinephrine (NE) concentration, and left stellate ganglion (LSG) neural activity were determined at baseline and after CSAD. We designed an AMI model by occluding the left anterior coronary artery, and performed analysis of VAs for 60 minutes using electrocardiography. Then, levels of c-fos and nerve growth factor (NGF) were determined.

Results: Relative to baseline values, CSAD prolonged ERP and APD of ventricles, increased HRV, decreased APD dispersion, BVR, ERP dispersion and serum NE concentration, and attenuated LSG activity in the CSAD group. AMI triggered a remarkable increase in LSG activity and function but decreased the HRV of the sham group animals relative to the CSAD group. Moreover, the CSAD group had higher levels of VAs relative to the sham group. This was accompanied by a corresponding decrease in proteins quantities of NGF and c-fos in the CSAD group in the LSG after AMI compared to the sham group.

Conclusions: CSAD can suppress LSG neural activity, hence enhance the electrophysiological stability and protect the heart from AMI-triggered VAs.

MeSH Keywords: **Afferent Pathways • Arrhythmias, Cardiac • Autonomic Nervous System • Myocardial Infarction • Sympathetic Nervous System**

Full-text PDF: <https://www.medscimonit.com/abstract/index/idArt/914105>

 3213

 1

 5

 32



Background

Lethal ventricular arrhythmias (VAs) often lead to sudden cardiac death, especially in patients suffering from ischemic heart diseases [1]. Ischemia-induced VAs have been shown to be caused by hyperactivity of the cardiac sympathetic nervous system [2]. Accordingly, various kinds of neuro-rebalance strategies that block excessive sympathetic activation have been shown to reduce the incidence of VAs and sudden cardiac death [3].

It is well known that acute myocardial infarction (AMI) induces the release of various metabolites that stimulate the cardiac sympathetic afferent nerve endings, resulting in increases in sympathetic nerve activity [4–6]. Previous studies have indicated that augmented cardiac sympathetic afferent reflex (CSAR) is a key contributor to enhanced sympathetic activity during ischemia, heart failure, and hypertension [7,8]. Recent functional evidence indicates that cardiac afferent fibers containing the transient receptor potential vanilloid 1 (TRPV1) have been implicated in the activation of CSAR. Selective deletion of these cardiac sympathetic afferents by application of resiniferatoxin (RTX), a compound capable of inducing rapid desensitization of TRPV1-expressing cardiac sympathetic afferent neurons and fibers by prolonging the opening of TRPV1-expression channels and increasing intracellular calcium within a short time frame, can almost absolutely abolish CSAR activation [9–12]. Given that a strategy for abolishing the augmented CSAR-induced sympathetic activation may be beneficial for protecting against the AMI-induced VAs, we investigated the potential protective effects of selective desensitization of TRPV1-expressing CSAR afferents on autonomic dysfunction and the ventricular electrophysiological characteristics and VAs during AMI.

Material and Methods

Animal preparation

All protocols for animal experimentation and the handling of animals were performed after approval from the Ethics Committee of our University (IACUC No. 20171224) and conformed to the principles described by the Guide for the Care and Use of Laboratory Animals of the National Institutes of Health (NIH publication 85-23, revised 1996). Mature male dogs (20.4±1.5 kg) were provided by the Department of Animals for Scientific Research, Renmin Hospital of Wuhan University and raised in the Laboratory Animal Centre of Wuhan University. One canine per cage were housed at 24±2°C conditions. Water and food were freely available. We used 3% Na-pentobarbital for anesthetization of 22 dogs at a starting dose of 1 mL/kg (intravenous) via dorsalis pedis vein. This was followed by ventilation of the animals with room air supplemented with oxygen using a positive pressure respirator. At intervals of 1 hour

during the operation, animals were given additional maintenance doses of 2 mg/kg (intravenous) of the same anesthesia through femoral vein sheath, using the corneal reflexes to assess the level of anesthesia. Fluid losses were compensated by injection of physiologic saline (50 to 100 mL/hour) through the femoral vein sheath. The dog's body temperature was kept at 36.5±1.5°C by a heating pad. A computer-based apparatus (Lead 7000, Jinjiang Inc., China) was applied for continuous recording of the body surface electrocardiogram (ECG) and arterial blood pressure (ABP) via the femoral arterial sheath. Left thoracotomy was performed at the fourth intercostal space. At the end of the experiment, the animals were not allowed to recover and euthanized with a lethal dose of sodium pentobarbital (150 mg/kg). All efforts were made to minimize the suffering of the dogs.

Experimental protocols

We allocated 22 dogs into 2 groups: cardiac sympathetic afferent denervation (CSAD) (n=9) and sham (sham operation without CSAD, n=13). CSAD was produced by epicardial application of RTX as previously described [10]. RTX and Tween 80 were supplied by Sigma-Aldrich (St. Louis, MO, USA). Briefly, RTX was solubilized in ethanol (2 mL) and mixed thoroughly with Tween in isotonic saline (2 mL of Tween 80 dissolved in 16 mL normal saline). The entire left and right ventricles were covered with medical skim gauze soaked with RTX (50 µg/mL) and the pericardium was sutured to ensure adequate drug contact and reduce drug losses. The vehicle (2 mL of absolute ethanol mixed thoroughly with 18 mL of Tween in isotonic saline) was applied to the epicardium as a control. Action potential duration (APD), APD dispersion, beat-to-beat variability of repolarization (BVR), heart rate variability (HRV), and ventricular effective refractory period (ERP), ERP dispersion, left stellate ganglion (LSG) neural activity and blood norepinephrine (NE) concentration were determined at baseline and 30 minutes after CSAD or sham intervention without CSAD. To establish an AMI model, the left anterior descending coronary artery was isolated and ligated below the first diagonal branch for 60 minutes. AMI was assessed by acute elevation of T-wave changes and ST-segment. Subsequently, the number of VAs during the first 60 minutes after AMI, LSG neural activity and function during AMI, serum NE level, ventricular ERP and APD, and HRV were continuously recorded (Figure 1). VAs were categorized as ventricular premature beats (VPBs), ventricular tachycardia (VT, ≥3 consecutive VPBs), and ventricular fibrillation (VF).

Measurements of HRV

Analysis of the overall activity of cardiac autonomic nervous system was based on HRV [13]. Spectral power of HRV was evaluated by 5-minute ECG data from baseline, 30 minutes after

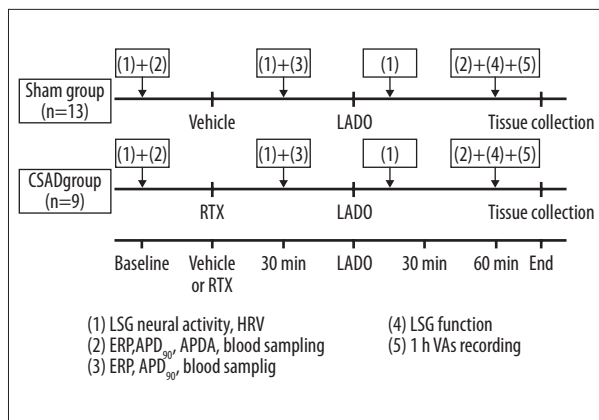


Figure 1. Experimental flow chart. Sham group, sham operation without cardiac sympathetic afferent denervation; CSAD group, with cardiac sympathetic afferent denervation; RTX – resiniferatoxin; LSG – left stellate ganglion; LADO – left anterior descending branch occlusion; ERP – effective refractory period; APD₉₀ – 90% repolarization duration; APDA – action potential duration alternans; HRV – heart rate variability; AMI – acute myocardial infarction; Vas – ventricular arrhythmias.

epicardial RTX or vehicle intervention, and 15 minutes after AMI; the digital ECG signals were used to analyze HRV spectral power via an autoregressive algorithm. The power spectral variables were defined as follows: from 0.04 to 0.15 Hz, low frequency component (LF); from 0.15 to 0.40 Hz, high frequency component (HF), and the ratio between LF and HF (LF/HF). The values of the HF and LF were examined and designated by normalized units (nu) according to a previous report [14].

Determination of ventricular ERP

Multielectrode catheters with a 2 mm interelectrode distance were inserted via 2 epicardial sites on free walls of the left ventricles. Measurement of the left ventricular ERP was performed from the ischemia area (IA, below the ligation site, near the left ventricular apex) and the ischemia remote area (IRA, near the left ventricular base). The ERP at each epicardial site was measured using a pacing protocol comprising of 8 consecutive stimuli (S1-S1, 300 ms cycle length), and then an extra stimulus (S2). To induced refractoriness, decrements of 10 ms followed by 2 ms were applied to reduce the S1-S2 interval from 250 ms [15]. ERP was considered as the longest S1-S2 interval that could not capture the ventricles. The dispersion of ERP was evaluated by a specific value (range/mean of ERP).

Measurement of monophasic action potentials (MAPs)

Left ventricular free walls MAPs were measured at IA and IRA via customized Ag-AgCl catheters in all animals. A dynamic steady-state pacing protocol (S1S1) was made to obtain MAP

duration and action potential duration alternans (APDA) cycle length. The pulse train was given at an initial cycle length which was shorter than the normal sinus cycle length followed by gradual shortening by 10 ms until APD alternans occurred. Each pulse train was delivered for at least 30 seconds to get a steady state, and the stimulation train was interrupted for 2 minutes to decrease the pacing memory effects before the next one was delivered. The MAP duration was evaluated at 90% repolarization (APD₉₀) under constant pacing cycle length (PCL) of 300 ms. The APDA was measured as the difference between APD₉₀ for 2 adjacent beats when the alternate APD₉₀ differed by 5% over 10 consecutive beats. The length of an APDA cycle was considered as the maximal PCL which induced APDA [15]. PowerLab data acquisition system (AD Instruments, Bella Vista, Australia) was used to acquire and analyze all MAPs signals. The bandwidth signal of the amplifier ranged from 0.3 Hz to 1000 Hz. APD₉₀ dispersion was calculated by the ratio (range/mean of APD₉₀). BVR for 30 consecutive beats was determined from the formula ($BVR = \sum |D_{N+1} - D_N| / [30 \times \sqrt{2}]$, where D represents the MAPs) [16].

LSG neural activity recording

LSG neural activity was determined for 60 seconds at 3 time points: baseline, 30 minutes after epicardial RTX or vehicle intervention, and 15 minutes after the AMI. The recording of neural electrical signals was performed by a tungsten-coated microelectrode inserted into the LSG and interference was reduced by a ground lead attached to the wall of the chest. All signals were amplified and filtered between 0.3 kHz and 1 kHz via a PowerLab system (AD Instruments, Bella Vista, Australia) as previously described [17]. LSG neural activity, estimated by the recorded frequency and amplitude from LSG, was defined as deflections with a signal-to-noise ratio greater than 3: 1. The increased frequency and amplitude from LSG imply an increase in LSG neural activity.

Assessment of LSG function

Responses to high-frequency stimulation of the LSG in terms of the highest change in systolic blood pressure (SBP) were used to assess LSG function as described previously [17]. High-frequency stimulation (from 10 V to 70 V, with increments of 10 V, 20 Hz, 0.1 ms pulse duration) was provided generated by the Grass-S88 stimulator. Thereafter, we plotted a voltage/SBP-response curve. The duration of each electrical stimulation was less than 30 seconds. A subsequent stimulation was only initiated when the BP values were restored to the baseline level.

Blood sampling

To determine the concentration of serum biomarkers from venous blood, serum NE concentration was measured with

Table 1. Effect of CSAD on heart rate and hemodynamic parameters.

	Heart rate (bpm)			Systolic BP (mm Hg)			Diastolic BP (mm Hg)		
	Baseline	30min	AMI	Baseline	30min	AMI	Baseline	30min	AMI
Sham group	140±19	138±12	142±15	138±18	136±8	107±15**	95±24	88±17	67±14*
CSAD group	137±14	130±13	135±16	141±22	132±13	125±25	87±22	84±19	77±21

Heart rate and blood pressure (BP) recordings between cardiac sympathetic afferent denervation (CSAD) group and sham group (sham operation without CASD) at baseline, 30 minutes after epicardial resiniferatoxin (RTX) or vehicle intervention (30 min), and 15 minutes after acute myocardial infarction (AMI). * $P < 0.05$ and ** $P < 0.01$ vs. group baseline

a Dog Norepinephrine ELISA kits (H096, Nanjing Jiancheng Bioengineering Inc, Nanjing, China).

Western blot

Fresh LSG tissues were excised at the end of the experiment and kept at -80°C . Western blot was applied to quantify the protein concentrations of NGF and c-fos from the LSG using anti-c-fos (ab156802, Abcam, Cambridge, UK) and anti-NGF (bs-10806R, Bioss, Beijing, China). The enhanced chemiluminescence system was used to visualize the separated protein bands. GAPDH served as the housekeeping protein (ab181603, Abcam, Cambridge, UK).

Data analysis

The continuous variables with normal distribution are shown as mean \pm standard deviation (SD). Comparisons among the variables before and after interventions were achieved by paired-samples *t*-test. The means of 2 groups after AMI 60 minutes were compared using independent-samples *t*-test. The non-parametric Wilcoxon signed ranks test and Mann-Whitney U test were applied for comparisons of the APDA cycle length. The Fisher exact test was applied to analyze the occurrence of VF between the 2 groups. The software SPSS 23.0 (IBM Corp., USA) was used for data analysis and 2-tailed $P < 0.05$ was considered significant.

Results

In this study, 5 dogs in the sham group and 1 dog in the CSAD group died of ventricular fibrillation after coronary artery ligation, and these dogs were not included in this study (except for the calculation of incidence of ventricular fibrillation).

Influence of CSAD on the hemodynamic parameters and heart rate

As shown in Table 1, ABP and heart rates were not altered at 30 minutes after CSAD. However, BP significantly decreased

after left anterior descending branch occlusion, and the decrease was attenuated in the CSAD group.

Effect of CSAD on VAs

Figure 2A illustrates the types of VAs triggered by acute myocardial infarction. Sixty minutes of continuous ECG recorded after AMI showed that the prevalence of VPB episodes were remarkably decreased in the CSAD group relative to sham group (Figure 2B). In addition, the incidence of VF and the episodes of VT were significantly lower, and mean duration of VT in the CSAD group was remarkably shorter relative to the sham group (Figure 2C–2E).

Influence of CSAD on ventricular electrophysiologic properties

Typical raw MAP signals from IA in the 2 groups are shown in Figure 3A. Compared to baseline, both ERP and APD_{90} were significantly prolonged by 30 minutes of CSAD treatment (Figure 3), yet no difference was observed in the sham group (Figure 3). Sixty minutes following left anterior descending branch occlusion, a marked reduction in ERP and APD_{90} from the IA was observed in the sham group, an effect that was prevented by CSAD (Figure 3D–3G). ERP and APD_{90} from the IRA were no significant differences after AMI in both groups (Figure 3E–3H). Compared to baseline, the marked elevation in ERP dispersion, APD_{90} dispersion and BVR was induced by AMI, which were significantly prevented in the CSAD group (Figure 3F, 3I–3K). AMI resulted in an elevation in APDA cycle length from the IA in the sham group, but this effect was suppressed in the CSAD group (Figure 3B).

Influence of CSAD on HRV

There were no remarkable changes in LF/HF, HF, and LF at baseline state in both groups. Thirty minutes later, LF/HF and LF were markedly decreased, and HF was markedly increased in the CSAD group, while no changes were recorded in the sham group. LF/HF and LF were increased while HF was decreased

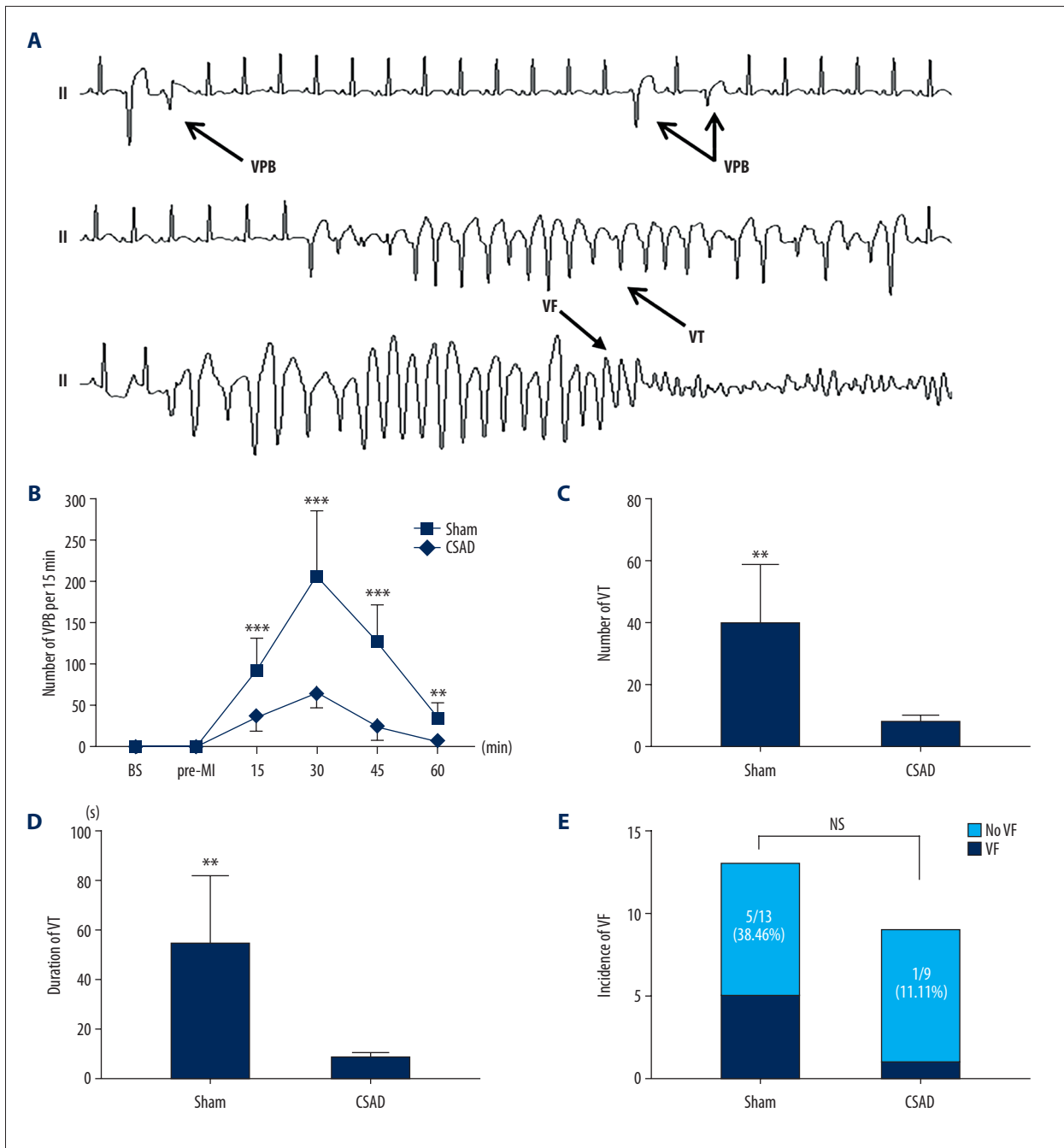


Figure 2. Effects of CSAD on VAs. (A) Representative AMI-induced ventricular arrhythmias. (B–E) The occurrence of the VAs in both groups. NS, $P>0.05$; ** $P<0.01$, and *** $P<0.001$ versus sham group. VPB – ventricular premature beat; VT – ventricular tachycardia; VF – ventricular fibrillation; BS – baseline. Other abbreviations as in Figure 1.

by AMI in the sham group, and these effects were absent in the CSAD group (Figure 4A–4C).

Impact of CSAD on serum NE concentration

After 30 minutes of CSAD treatment, serum NE level was remarkably reduced in the CSAD group, while the change of

serum NE level at baseline and after sham operation were similar. AMI increased the serum NE concentration in the sham group, but not in the CSAD group (Figure 4D).

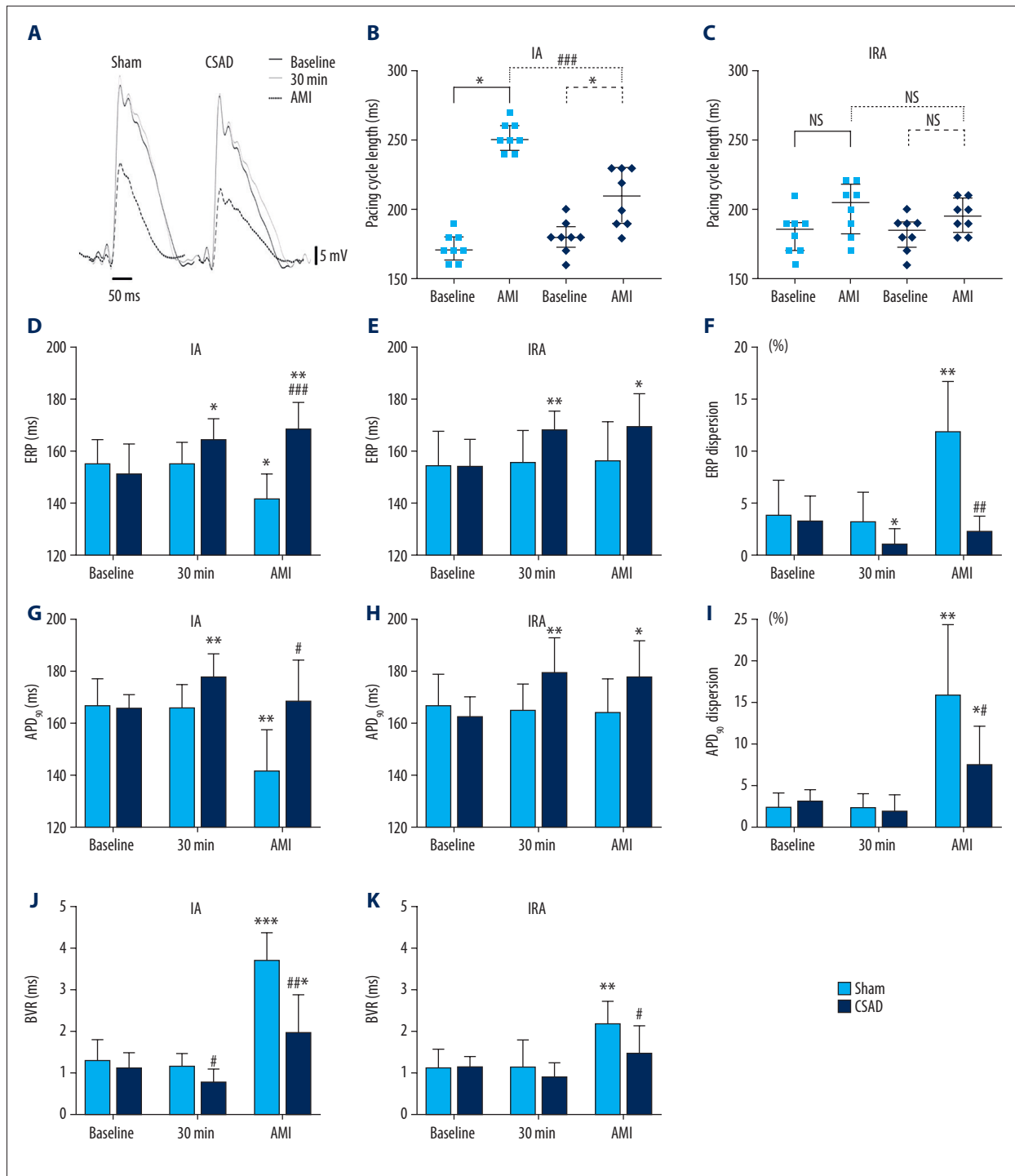


Figure 3. Effect of CSAD on ventricular electrophysiological properties. (A) Representative examples of MAP from the IA in the both groups. (B–K) The changes in ERP, APD₉₀, ERP dispersion, APD₉₀ dispersion, beat-to-beat variability of repolarization and APD₉₀ cycle length in both groups at baseline, 30 minutes after epicardial RTX or vehicle intervention (30min), and 60 minutes after acute myocardial infarction (AMI). NS, $P > 0.05$; * $P < 0.05$, ** $P < 0.01$, and *** $P < 0.001$ versus group baseline; # $P < 0.05$, ## $P < 0.01$, and ### $P < 0.001$ versus sham group. IA – ischemia area; IRA – ischemia remote area; BVR – beat-to-beat variability of repolarization. Other abbreviations as in Figure 1.

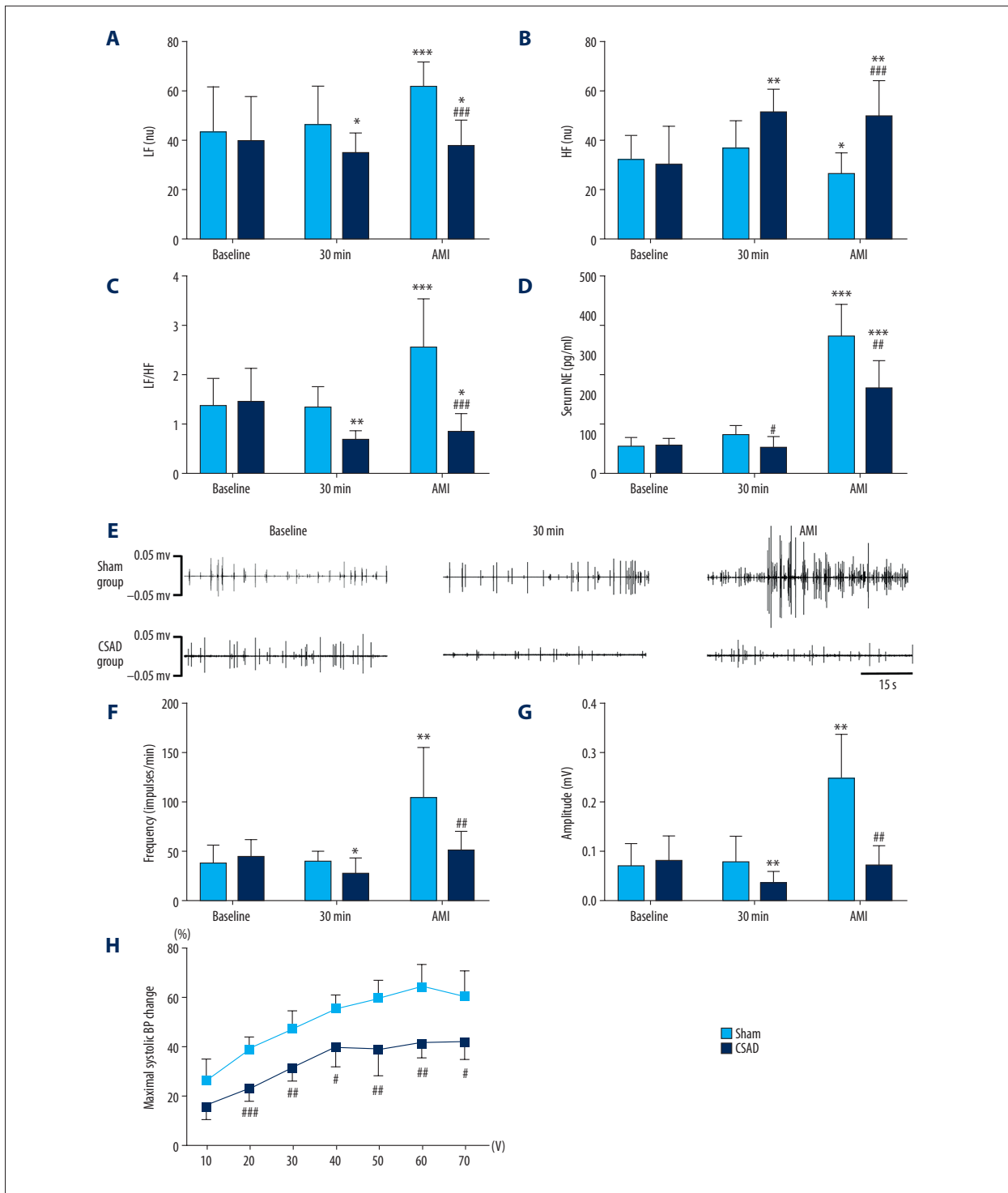


Figure 4. Effect of CSAD on cardiac autonomic nervous activity. (A–C) The changes in HRV between 2 groups at baseline, 30 minutes after epicardial RTX or vehicle intervention (30 min), and 15 minutes after acute myocardial infarction (AMI). (D) Effect of LADO and CSAD on serum norepinephrine (NE) at baseline, 30 minutes after intervention (30 min), and 60 minutes after acute myocardial infarction (AMI). (E–G) Typical images and the quantitative analysis of the LSG neural activity at each time points in the 2 groups. (H) Effect of CSAD on LSG function at the same time point. * $P < 0.05$, ** $P < 0.01$, and *** $P < 0.001$ versus group baseline; # $P < 0.05$, ## $P < 0.01$, and ### $P < 0.001$ versus sham group. HF – high frequency; LF – low frequency; LF/HF – ratio between LF and HF. Other abbreviations as in Figure 1.

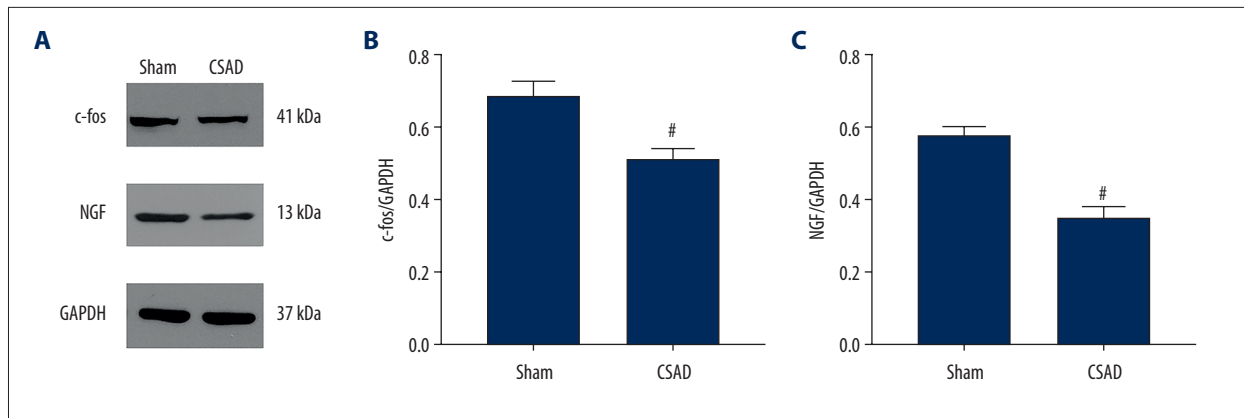


Figure 5. Effect of CSAD on c-fos and nerve growth factor (NGF) protein expression. (A) Representative western blot images, and (B, C) quantitative analyses of the expressions of c-fos and NGF in LSG in both groups. # $P < 0.05$ versus sham group. Other abbreviations as in Figure 1.

The impact of CSAD on LSG activity and function

Figure 4E illustrates the representative neural activity images from LSG recorded at baseline, 30 minutes after CSAD or sham operation, and 15 minutes after AMI for 1 minute between the 2 groups. Quantitative analysis indicated that both the amplitude and frequency of the neural activity obtained from the LSG were significantly decreased at 30 minutes after CSAD treatment in the CSAD group, whereas the changes in the neural activity after sham operation and at baseline were similar. Compared to baseline, AMI triggered a remarkable rise in the amplitude and frequency of the neural activity recorded from the LSG in the sham group, but not in the CSAD group (Figure 4F, 4G). Maximal SBP change caused by LSG direct electrical stimulation at 60 minutes after AMI between the 2 groups is summarized in Figure 4H. The change of maximal SBP was obviously prevented during LSG stimulation in the CSAD group relative to the sham group.

Effect of CSAD on NGF and c-fos protein expression

Typical western blots of c-fos and NGF are shown in Figure 5A. Quantitative results indicate that AMI decreased NGF and c-fos proteins in the LSG in the CSAD group compared with the sham group (Figure 5B, 5C).

Discussion

The findings of this study evidently demonstrated that CSAD enhanced ventricular electrophysiological stability and protected the heart against AMI-induced VAs in canines. Mechanistically, we propose that the anti-arrhythmic effect of CSAD is mediated by modulating cardiac sympathetic nerve activity.

Basic and clinical studies have suggested that increased cardiac sympathetic nerve activity is thought to contribute to VAs [18–21]. It is well known that AMI releases various metabolites including ATP, protons, bradykinin, and histamine that stimulate cardiac sympathetic afferent nerve endings and lead to an activation of sympathetic nerve activity [22]. Here, we provide direct evidence that CSAD by epicardial treatment of RTX attenuates cardiac sympathetic nerve during AMI in canines: First, in the CSAD group, LF (nu) and LF/HF at 30 minutes after RTX application were remarkably reduced relative to the sham group, and the AMI-induced increases of LF (nu) and LF/HF were markedly suppressed by RTX. Second, LSG neural activity and function were significantly attenuated by RTX. Third, RTX significantly attenuated AMI-induced increase of serum NE level. These findings indicate a vital role of the CSAR to the augmented cardiac sympathetic activity during AMI.

Previous studies have demonstrated that cardiac electrophysiological properties are influenced by cardiac autonomic nervous system. Additionally, it has been shown that sympathetic stimulation shortens ventricular APD, ERP and increases dispersion of repolarization, while sympathetic denervation protects them [23–25]. Here, we found that both ventricular ERP and APD were significantly prolonged by CSAD treatment. CSAD treatment also decreased the dispersion of ERP and APD induced by AMI. The APD restitution hypothesis indicates that the steep restitution slope is relevant with unstable dynamics, easier to cause wave break-ups and conduction blocks that promote initiation and maintenance of VF, while the flattened restitution curve suggests a cardioprotective effect [26]. The occurrence of APD alternans, an indicator of malignant VAs, is higher with the steeply sloped restitution curves [27]. A delayed APD alternans is correlated with a low risk of malignant VAs. Our study showed that CSAD shortens APD alternans cycle length. Lability of repolarization, providing valuable information to assess the susceptibility to proarrhythmia, can be

used as a predictive parameter for lethal VAs [16]. The occurrence of malignant VAs was associated with the increase in BVR of MAPs. The increase of BVR after AMI can be inhibited by CSAD in this study. Therefore, the CSAD-mediated arrhythmic effect is potentially through increasing ventricular electrophysiological stability.

The sympathetic dynamic change is associated with altered neuropeptides and neurotransmitters. In this study, we measured the protein expression of NGF and c-fos to provide mechanistic explanation. NGF is known to be expressed in the heart and other sympathetic targets, and determines the density of innervation by the sympathetic nervous system [28]. Prior experiments have suggested that NGF facilitates LSG remodeling and is thought to contribute to the increased ischemia-related VAs [29,30]. In this study, we detected protein expression of NGF from the LSG after AMI, and found that CSAD attenuated the NGF expression levels. C-fos, a third messenger, is often expressed rapidly in neurons after stimulation, and used as an important biomarker for fast neuronal activation [31]. Our study showed that c-fos expression was significantly downregulated by CSAD. Therefore, it is possible that CSAD inhibits the LSG neural activity and function by regulating the concentration of neurotransmitters and/or neuropeptides. However, the precise mechanism underlying the regulation of neurotransmitters and/or neuromodulators by CSAD is unclear. A previous study suggested that the increased pro-inflammatory cytokines in spontaneously hypertensive rats mediated an increase in cardiac sympathetic afferent reflex and sympathetic outflow [32]. The Wang et al. study showed that increased inflammation promoted the expression of neuromodulators and regulated the remodeling of LSG [30]. Therefore, it is more likely that RTX impacts afferent drive to the LSG through the central nervous system to mitigate sympathetic output.

Nevertheless, the following issues need to be considered in this study. First, the use of pentobarbital for anesthetization may affect the autonomic nervous system. But this effect may have had little influence since pentobarbital was given continuously throughout the entire operation and implemented using similar protocols in all study animals. Second, we only observed the effect of CSAD in an AMI model, the long-term effect of CSAD on cardiac electrophysiology was not examined. Third, cardiac function is an important factor for ischemia-induced ventricular arrhythmias. However, we didn't measure the left ventricle pressure directly. However, the change of blood pressure reflects the function of left ventricle to some extent. Fourth, the assessment of APDA occurrence by a fixed percentage might be inaccurate and might pick up non-alternans variability. However, this could have been mitigated due to the familiar method that was implemented in both groups. Finally, the data of this study suggests that epicardial administration of RTX affects cardiac electrophysiology by modulating cardiac autonomic nervous system. However, we didn't completely exclude the possibility that RTX might directly affect cardiac electrophysiology.

Conclusions

In the present study, we provided evidence that CSAD improved the cardiac electrophysiology stability and protected the heart against AMI-induced Vas in an animal model. The decreased LSG activity and function, in part due to the reduced c-fos and NGF levels in the LSG, contributed to the protective function of CSAD against AMI-induced VAs. CSAD might be a novel strategy to prevent AMI-induced VAs.

Conflicts of interest

None.

References:

- Buxton AE: Sudden death in ischemic heart disease – 2017. *Int J Cardiol*, 2017; 237: 64–66
- Shen MJ, Zipes DP: Role of the autonomic nervous system in modulating cardiac arrhythmias. *Circ Res*, 2014; 114: 1004–21
- Hou Y, Zhou Q, Po SS: Neuromodulation for cardiac arrhythmia. *Heart Rhythm*, 2016; 13: 584–92
- Malliani A, Montano N: Emerging excitatory role of cardiovascular sympathetic afferents in pathophysiological conditions. *Hypertension*, 2002; 39: 63–68
- Fu LW, Guo ZL, Longhurst JC: Endogenous endothelin stimulates cardiac sympathetic afferents during ischaemia. *J Physiol*, 2010; 588: 2473–86
- Fu LW, Longhurst JC: A new function for ATP: Activating cardiac sympathetic afferents during myocardial ischemia. *Am J Physiol Heart Circ Physiol*, 2010; 299: H1762–71
- Thames MD, Kinugawa T, Dibner-Dunlap ME: Reflex sympathoexcitation by cardiac sympathetic afferents during myocardial ischemia. Role of adenosine. *Circulation*, 1993; 87: 1698–704
- Chen WW, Xiong XQ, Chen Q et al: Cardiac sympathetic afferent reflex and its implications for sympathetic activation in chronic heart failure and hypertension. *Acta Physiol*, 2015; 213: 778–94
- Zahner M, Li D, Chen S, Pan H: Cardiac vanilloid receptor 1-expressing afferent nerves and their role in the cardiogenic sympathetic reflex in rats. *J Physiol*, 2003; 551: 515–23
- Wang HJ, Wang W, Cornish KG et al: Cardiac sympathetic afferent denervation attenuates cardiac remodeling and improves cardiovascular dysfunction in rats with heart failure. *Hypertension*, 2014; 64: 745–55
- Sun H, Li DP, Chen SR et al: Sensing of blood pressure increase by transient receptor potential vanilloid 1 receptors on baroreceptors. *J Pharmacol Exp Ther*, 2009; 331: 851–59
- Olah Z, Szabo T, Karai L et al: Ligand-induced dynamic membrane changes and cell deletion conferred by vanilloid receptor 1. *J Biol Chem*, 2001; 276: 11021–30
- Camm AJ, Malik M, Bigger JT et al: Heart rate variability. Standards of measurement, physiological interpretation, and clinical use. *Eur Heart J*, 1996; 17: 354–81

14. Xiong L, Liu Y, Zhou M et al: Targeted ablation of cardiac sympathetic neurons improves ventricular electrical remodeling in a canine model of chronic myocardial infarction. *Europace*, 2018; 20(12): 2036–44
15. He B, Lu Z, He W et al: Effects of ganglionated plexi ablation on ventricular electrophysiological properties in normal hearts and after acute myocardial ischemia. *Int J Cardiol*, 2013; 168: 86–93
16. Gallacher DJ, André DW, Henk DL et al: *In vivo* mechanisms precipitating torsades de pointes in a canine model of drug-induced long-QT1 syndrome. *Cardiovasc Res*, 2007; 76: 247–56
17. Wang S, Zhou X, Huang B et al: Spinal cord stimulation protects against ventricular arrhythmias by suppressing left stellate ganglion neural activity in an acute myocardial infarction canine model. *Heart Rhythm*, 2015; 12: 1628–35
18. Jardine DL, Charles CJ, Frampton CM, Richards A: Cardiac sympathetic nerve activity and ventricular fibrillation during acute myocardial infarction in a conscious sheep model. *Am J Physiol Heart Circ Physiol*, 2007; 293: H433–39
19. Doytchinova A, Patel J, Zhou S et al: Subcutaneous nerve activity and spontaneous ventricular arrhythmias in ambulatory dogs. *Heart Rhythm*, 2015; 12: 612–20
20. Doytchinova A, Hassel JL, Yuan Y et al: Simultaneous noninvasive recording of skin sympathetic nerve activity and electrocardiogram. *Heart Rhythm*, 2017; 14: 25–33
21. Shen MJ, Coffey AC, Straka S et al: Simultaneous recordings of intrinsic cardiac nerve activity and skin sympathetic nerve activity from human patients during the postoperative period. *Heart Rhythm*, 2017; 14: 1587–93
22. Fu L, Longhurst J: Regulation of cardiac afferent excitability in ischemia. *Handb Exp Pharmacol*, 2009; 194: 185–225
23. Ng G, Brack K, Patel V, Coote J: Autonomic modulation of electrical restitution, alternans and ventricular fibrillation initiation in the isolated heart. *Cardiovasc Res*, 2007; 73: 750–60
24. Huang B, Yu L, He B et al: Sympathetic denervation of heart and kidney induces similar effects on ventricular electrophysiological properties. *EuroIntervention*, 2015; 11: 598–604
25. Jungen C, Gogh GV, Schmitt C et al: Mismatch between cardiac perfusion, sympathetic innervation, and left ventricular electroanatomical map in a patient with recurrent ventricular tachycardia. *Am J Case Rep*, 2016; 17: 280–82
26. Weiss JN, Chen PS, Qu Z et al: Electrical restitution and cardiac fibrillation. *J Cardiovasc Electrophysiol*, 2002; 13: 292–95
27. Weiss JN, Qu Z, Chen PS et al: The dynamics of cardiac fibrillation. *Circulation*, 2005; 112: 1232–40
28. Zhou S, Chen LS, Miyauchi Y et al: Mechanisms of cardiac nerve sprouting after myocardial infarction in dogs. *Circ Res*, 2004; 95: 76–83
29. Huang B, Yu L, Scherlag BJ et al: Left renal nerves stimulation facilitates ischemia-induced ventricular arrhythmia by increasing nerve activity of left stellate ganglion. *J Cardiovasc Electrophysiol*, 2014; 25: 1249–56
30. Wang M, Li S, Zhou X et al: Increased inflammation promotes ventricular arrhythmia through aggravating left stellate ganglion remodeling in a canine ischemia model. *Int J Cardiol*, 2017; 248: 286–93
31. Sagar S, Sharp F, Curran T: Expression of c-fos protein in brain: Metabolic mapping at the cellular level. *Science*, 1988; 240: 1328–31
32. Shi Z, Jiang SJ, Wang GH et al: Pro-inflammatory cytokines in paraventricular nucleus mediate the cardiac sympathetic afferent reflex in hypertension. *Autonomic Neuroscience*, 2014; 186: 54–61